

# Low Birefringence and 2-D Optical Confinement of Hollow Waveguide With Distributed Bragg Reflector and High-Index-Contrast Grating

Volume 1, Number 2, August 2009

Mukesh Kumar, Student Member, IEEE

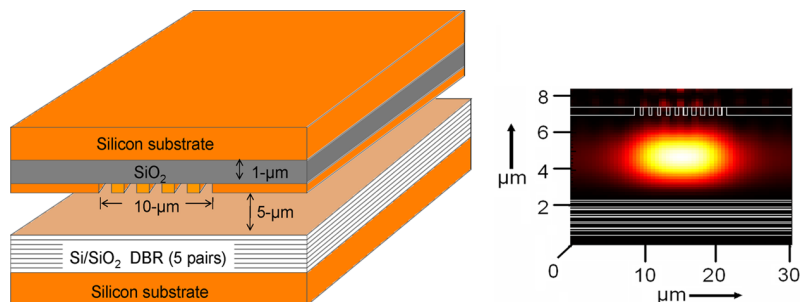
Chris Chase, Student Member, IEEE

Vadim Karagodsky

Takahiro Sakaguchi

Fumio Koyama, Fellow, IEEE

Connie J. Chang-Hasnain, Fellow, IEEE



DOI: 10.1109/JPHOT.2009.2027027

1943-0655/\$26.00 ©2009 IEEE

# Low Birefringence and 2-D Optical Confinement of Hollow Waveguide With Distributed Bragg Reflector and High-Index-Contrast Grating

Mukesh Kumar,<sup>1</sup> *Student Member, IEEE*, Chris Chase,<sup>2</sup> *Student Member, IEEE*, Vadim Karagodsky,<sup>2</sup> Takahiro Sakaguchi,<sup>1</sup> Fumio Koyama,<sup>1</sup> *Fellow, IEEE*, and Connie J. Chang-Hasnain,<sup>2</sup> *Fellow, IEEE*

<sup>1</sup>Microsystem Research Center, Tokyo Institute of Technology, Yokohama 226-8503, Japan

<sup>2</sup>Department of Electrical Engineering and Computer Sciences, University of California at Berkeley, Berkeley, CA 94720 USA

DOI: 10.1109/JPHOT.2009.2027027  
1943-0655/\$26.00 © 2009 IEEE

Manuscript received May 29, 2009; revised June 24, 2009. First published Online July 7, 2009. Current version published July 29, 2009. This work is supported by Photonics Integration—Core Electronics (PICE) program under the Global-COE of Ministry of Education of Japan and by the Center for Integrated Access Networks (CIAN) sponsored by the National Science Foundation. Corresponding author: Mukesh Kumar (e-mail: kumar.m.aa@m.titech.ac.jp).

**Abstract:** A hollow optical waveguide is proposed in which light can be confined in an air gap between a distributed Bragg reflecting (DBR) mirror and a high-index-contrast grating (HCG) mirror. Because of the combined effect of vertical (DBR) and lateral (HCG) periodicity, the proposed hollow waveguide shows a small modal birefringence on the order of  $10^{-4}$ . In addition, a patterned HCG is shown to provide 2-D optical confinement, which is an important requirement for practical compact photonic devices. The proposed hollow waveguide is fabricated, and a low birefringence of  $5 \times 10^{-4}$  is demonstrated experimentally.

**Index Terms:** Integrated photonics, waveguides, gratings, optical devices.

## 1. Introduction

Hollow optical waveguides have been attracting much attention for various applications in including sensing for clinical, industrial, and environmental applications [1]–[4], spectroscopy [5] and optical communications [6]. A novel concept for guiding light in a core with a refractive index lower than that of cladding was proposed in form of Bragg fibers [7], Omni waveguides [8] and antiresonant reflecting optical waveguides (ARROWs) [9]. Attenuation and nonlinearities resulting from the interaction of light with the dense, material-filled core in conventional dielectric waveguides can be circumvented by confining light in an air core using highly reflective walls [10]. Temperature insensitivity and wide tuning are two inherent characteristics of hollow waveguides (HWGs) [11] which can be utilized to make widely tunable photonic devices without any need of temperature controllers.

Design flexibility of HWGs is a key to build the photonic devices with various functionalities [12]–[14]. Strong vertical optical confinement in HWGs can be achieved using top and bottom distributed Bragg reflectors (DBRs) as cladding, having quarter-wavelength-thick layers designed for oblique incidence of light [15], where light is guided in the air gap in between the two DBRs. The reflectivity of DBRs in the HWG is highly polarization dependent because of the periodicity only in one direction which is  $Y$ -direction in our case. Usually, the complex geometries support TE-like and TM-like modes, but for convention we call them TE and TM modes. The polarization is TM if the

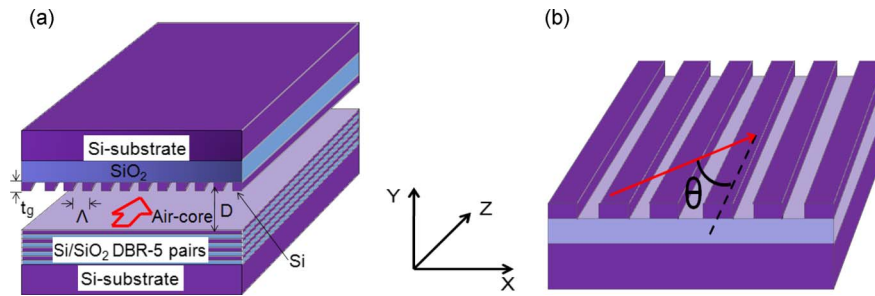


Fig. 1. Schematic of (a) HWG consisting of a DBR mirror and an HCG mirror and (b) HCG with YZ plane being plane of incidence. Z is the propagation direction.

E-field lies in Y-direction i.e., parallel to the direction of periodicity in DBR (we call it vertical periodicity) and perpendicular to the direction of propagation (Z). While for TE polarization, the E-field lies in X-direction, we call it lateral direction. Due to a larger field penetration into the DBRs for TM mode than TE mode, the propagation constant  $\beta_{\text{TM}}$  is larger than  $\beta_{\text{TE}}$  and hence resulting in a significant birefringence. The polarization dependence of a HWG becomes very large at a narrow air core [16] where a HWG offers giant tuning of over 10% in propagation constant [11]. However, for many applications, it is desirable to have a low birefringence. In this paper, we propose and demonstrate a novel HWG structure with a very low birefringence.

We began by noting that the birefringence of the HWG largely comes from the guiding DBR having periodicity only in the one direction. If a lateral periodicity (perpendicular to both, the direction of propagation and the direction of DBR periodicity) is introduced in the HWG, the polarization dependence of the HWG can be reduced. High-reflectivity DBRs can be replaced with a high-index-contrast grating (HCG) mirror which gives broadband high reflection [17]–[18]. Recently, HCG HWGs were proposed to achieve an extremely low loss ( $< 0.01$  dB/m) [19]. The HCG mirror can be introduced, as a lateral periodicity, in HWGs to reduce its birefringence. The combined (and opposite) effect of DBR (vertical periodicity) and HCG (lateral periodicity) enable us to reduce birefringence even at a narrow air core. Important issues are how to realize low-loss 3-D HWGs and how to increase the design flexibility in their polarization dependence. The introduction of HCG into HWGs can extend the fabrication tolerance of the structure because of the large fabrication tolerance of HCG [17]. Also, because of the ease of fabrication of HCG, it is possible to design it for one particular polarization, making polarization control very flexible. With the flexibility of HCG design, it is possible to build HWGs with widely tunable polarization nature for variety of applications.

In this paper, an HWG with vertical and lateral periodicity is proposed which consists of a DBR mirror as vertical periodicity and an HCG mirror as lateral periodicity. We show that the combination of DBR and HCG mirrors can provide strong optical confinement and can reduce the birefringence of the HWG with narrow air cores. Also, it is possible to achieve the 2-D confinement by simply reducing the width of the HCG, which can lead to a cost-effective waveguide fabrication. The full-vector simulations of HCG and HWG, based on Rigorous coupled wave analysis (RCWA) [20], Finite-Difference Method (FDM) and Film-Mode-Matching Method (FMMM) [21] are presented. We experimentally demonstrate a low propagation loss for a TE mode and a low birefringence in an HWG with vertical and lateral periodicity.

## 2. Structure of Proposed HWG

The schematic of the proposed HWG is shown in Fig. 1. It consists of a DBR as a bottom mirror and an HCG as a top mirror of an HWG. Light can be confined vertically in an air core utilizing the high reflectivities of DBR and HCG. The structure consists of a 5-pair Si/SiO<sub>2</sub> bottom DBR mirror where each layer in DBR is quarter-wavelength thick, which is designed for oblique incidence. Because of the high refractive index contrast between Si and SiO<sub>2</sub>, only 5 pairs of Si/SiO<sub>2</sub> are enough to achieve a high reflectivity. The top HCG mirror consists of a high-index-contrast silicon/air grating. In an HCG mirror, many in-plane reflections add up and give rise to vertical high reflection [17]. The

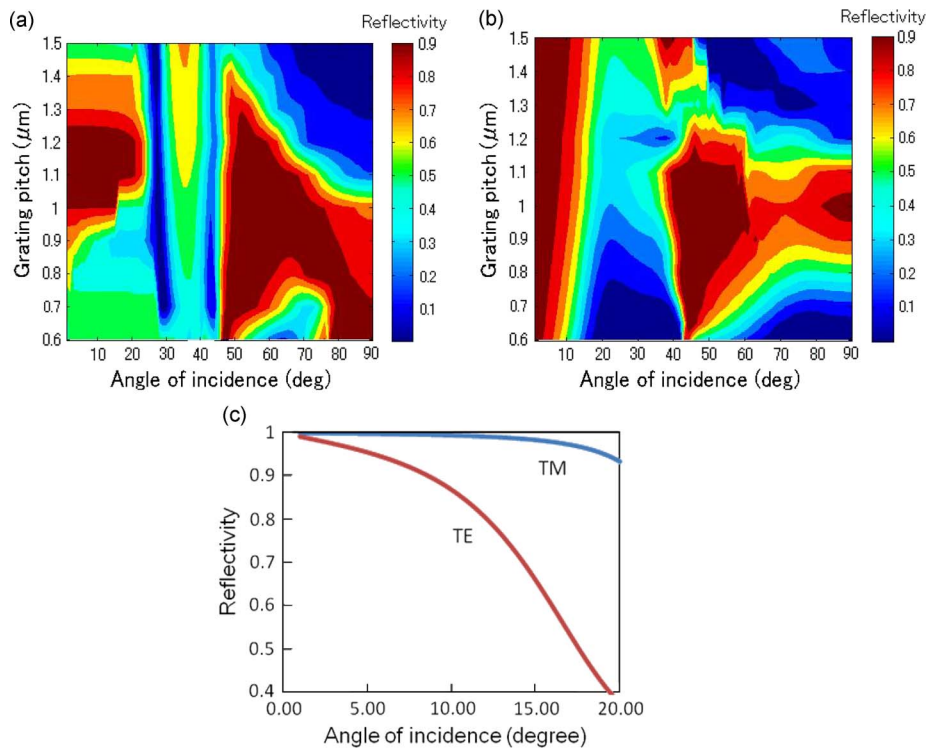


Fig. 2. Effect of pitch and angle of incidence on HCG reflectivity for (a) TM mode and (b) TE mode and (c) reflectivity versus angle of incidence at grating thickness  $t_g = 0.45 \mu\text{m}$ , grating pitch  $\Lambda = 1.2 \mu\text{m}$ , and duty cycle  $C = 0.41$ .

important design criterion for the HCG is that the transmitted waves should interfere destructively and the waveguiding inside the grating should also be avoided by optimizing the grating parameters. The important design parameters for the HWGs are: air-core thickness  $D$ , grating thickness  $t_g$ , grating pitch  $\Lambda$ , grating teeth width  $w$  and grating duty cycle  $C$ . In an HWG, the angle of incidence of optical rays will be small. To confine the light in air, one of the important requirements is to design the HCG at oblique incidence. In the following section, we study the dependence of HCG reflectivity on the angle of incidence.

### 3. HCG: Incidence Angle Dependence

In an HWG, the complementary angle of incidence, shown in Fig. 1(b), remains small. The analysis of incidence angle dependence of HCG reflectivity becomes important to find the optimized grating parameters to achieve high reflectivity from HCG at oblique incidence. As shown in Fig. 1(b), the plane of incidence, in the proposed HWG, is YZ. Fig. 2(a) and (b) show the dependence of reflectivity for TM and TE modes on an incidence angle in YZ plane and on the grating pitch; where grating thickness  $t_g = 0.45 \mu\text{m}$ , grating teeth width  $w = 0.5 \mu\text{m}$  and a wavelength of 1550 nm has been assumed. For these parameters, the required grating pitch, to achieve high reflectivity, for oblique incidence ( $\theta \sim 10^\circ$ ) of TM mode is larger than that for normal incidence ( $\theta \sim 90^\circ$ ). In going from normal to oblique incidence, the diffraction loss increases because of the de-phasing in laterally excited modes and one needs larger pitch (or smaller duty cycle) to reduce the diffraction losses. In case of TE mode also, larger pitch is required to achieve high reflectivity at oblique incidence. For application in HWGs, we need to consider only oblique incidence. Fig. 2(c) shows the calculated reflectivity of HCG versus the angle of incidence for TE and TM modes at  $t_g = 0.45 \mu\text{m}$ , grating pitch  $\Lambda = 1.2 \mu\text{m}$  and grating duty cycle  $C = 0.41$ . The simulation has been done using RCWA. The reflectivity of TM mode is larger than that of TE modes at all angles which shows that the penetration of TE mode into cladding is larger than that of TM mode. For the angle of

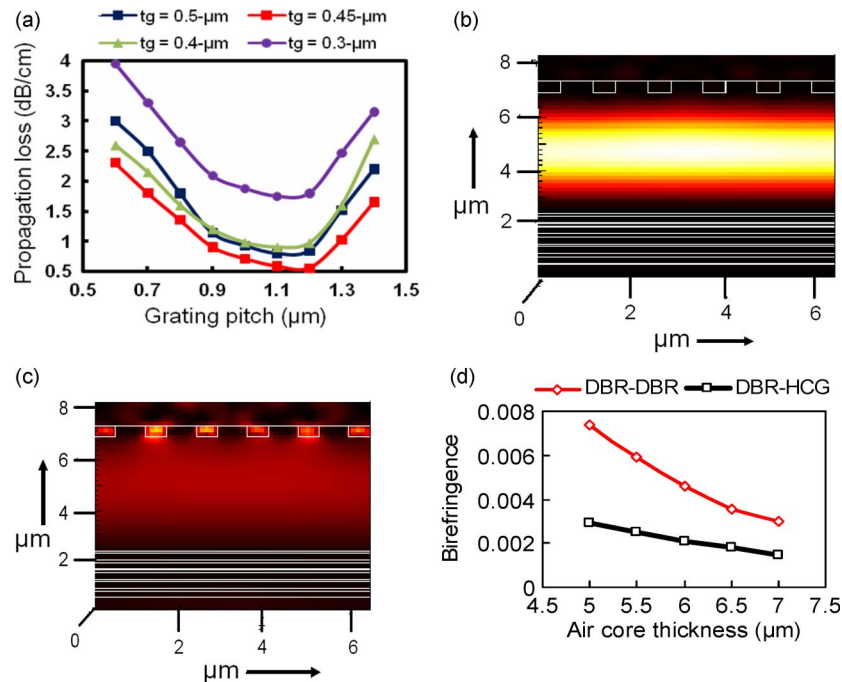


Fig. 3. (a) Computed effect of grating pitch  $\Lambda$  and grating thickness  $t_g$  on propagation loss of TE mode at grating teeth width of  $0.5 \mu\text{m}$  and air-core thickness  $D = 5 \mu\text{m}$ , (b) and (c) computed mode field distributions, respectively, for TE and TM modes, at the parameters of set A, and (d) birefringence as a function of  $D$  at the grating parameters in “set A”; birefringence of HWG with DBR on the both sides is also shown.

incidence around  $8^\circ$ , which is the case of HWG at an air-core thickness of  $5 \mu\text{m}$ , the reflectivity of TM mode is 99.8% while it is 94% for TE mode.

#### 4. Propagation Characteristics of HWG

The high reflectivity of a bottom DBR mirror and that of a top HCG mirror in our proposed HWG can be utilized to confine light in the air gap between the two mirrors. The basic schematic of the proposed HWG with vertical and lateral periodicity was shown in Fig. 1(a). The simulation of HWG has been performed using FMMM and is confirmed by FDM. The effect of grating pitch  $\Lambda$  and grating thickness  $t_g$  on the propagation loss for a fundamental TE mode, computed by FMMM, is shown in Fig. 3(a). For the simulation, the wavelength of  $1.55 \mu\text{m}$  has been chosen. The air-core thickness of the HWG is  $5 \mu\text{m}$  and the grating teeth width is  $0.5 \mu\text{m}$ . It is shown that the propagation loss of the HCG HWG is sensitive to any change in  $\Lambda$  and  $t_g$ . Low propagation loss can be realized with a larger pitch (low duty cycle) of the grating even at narrower air cores. At any  $t_g$ , the propagation loss has a minimum near a pitch of  $\Lambda = 1.2 \mu\text{m}$ . The propagation loss is lowest for  $t_g = 0.45 \mu\text{m}$ . The lowest calculated propagation loss at  $\Lambda = 1.2 \mu\text{m}$ ,  $C = 0.41$  and  $t_g = 0.45 \mu\text{m}$  is 0.55 dB/cm at an air-core thickness of  $5 \mu\text{m}$  which is acceptable for millimeter-long waveguide devices. The set of the optimized parameters with  $D = 5 \mu\text{m}$ ,  $t_g = 0.45 \mu\text{m}$ ,  $\Lambda = 1.2 \mu\text{m}$ ,  $w = 0.5 \mu\text{m}$  and  $C = 0.41$  is called “set A” for convenience. It is noted that for oblique incidence, which is the case with HWGs, one needs larger pitch or smaller duty cycle of HCG to achieve low-loss HWGs. For the same parameters, the propagation loss of the TM mode is 2.7 dB/cm. The calculated mode field distributions of TE and TM modes in the HWG with vertical and lateral periodicity are shown in Fig. 3(b) and (c), respectively. We note the strong vertical confinement in the HWG and the confinement of the TE mode is stronger than that of the TM mode. In HWGs, higher order modes exist but if a fundamental mode is excited then it will be retained efficiently.

HWGs show large polarization dependence because of the shallow incidence angle of a fundamental mode. To realize ultrawide tuning in HWGs, we need to use an HWG with a narrower

air core; but the birefringence at narrower cores remains large [16]. The polarization characteristics of HCG HWGs are shown in terms of birefringence in Fig. 3(d) at the grating parameters of “set A.” The birefringence is defined as  $B = (\beta_{TE} - \beta_{TM})/\beta_{TE}$ , where  $\beta$  is propagation constant. In Fig. 3(d), the effect of an air core on the birefringence is shown where the birefringence of conventional HWGs (having DBRs on top and bottom) is also shown for comparison. The result shows that the birefringence of the HCG HWG is much smaller than that of the conventional HWG at narrower air cores. By increasing the air-core thickness, the birefringence of the HWGs decreases for both the cases [16]. At an air-core thickness of  $5 \mu\text{m}$ , the birefringence of the HCG HWG is  $2.8 \times 10^{-3}$ ; which is almost 2.6 times smaller than the birefringence of a conventional HWG. To achieve ultrawide tuning, the HCG HWG with narrower air cores can be realized with smaller birefringence. The reason for this small birefringence is because of the opposite nature of conventional DBR mirror and HCG mirror; their combined (and opposite) interaction with the orthogonal polarizations results in the reduced birefringence. In case of the DBR-DBR HWG, the large birefringence comes from the field penetration of a TM mode into the DBR. The propagation constant of a TM mode is larger than that of a TE mode. On the other hand, a HCG gives us stronger optical confinement for a TM mode in an air core than DBRs. Thus, the propagation constant of a TM mode in the HCG-DBR HWG is smaller than that in the DBR-DBR HWG while the propagation constant of a TE mode remains almost same for both the cases. The difference in the field penetration results in a lower birefringence.

## 5. Two-Dimensional Confinement With Patterned HCG

For the implementation of HWGs in practical photonic devices, it is necessary to confine light in the lateral direction. As we have seen in the above discussion, a strong vertical confinement can be achieved in an HWG with a HCG mirror which is shown in Fig. 3(b). Two-dimensional optical confinement in HWGs can be achieved by increasing the effective index of the air core in the middle of the air-core region. This can be done by introducing the HCG only in the middle region as shown in Fig. 4(a), where the effective index of the fundamental mode in the middle of air core is  $n_1$  while the effective index of rest of the air core is  $n_2$ . We found that the presence of HCG increases the effective index of the fundamental guided mode causing  $n_1 > n_2$ , which provides strong lateral optical confinement because of the quasi-total internal reflection [13]. Fig. 4(b) and (c) show the calculated field distributions for TE and TM modes, respectively, where vertical and lateral optical confinement is noted. The simulation has been done using FMMM. The width of the grating region in the top HCG mirror is  $10 \mu\text{m}$ ; where the parameters of “set A” are used. The calculated effective index  $n_1$  under the HCG is larger than that ( $n_2$ ) of the outside cladding region. The vertical confinement in the absence of HCG results from the antiresonant reflection because of the index discontinuity and the glancing angle of incidence, owing to the principle from ARROW structures [9]. The larger effective index under HCG is because of the fact that the multi-reflections from HCG increase the phase difference of the guided light which increases the effective index. Therefore, 2-D confinement can be realized by introducing a patterned HCG in the middle.

The calculated propagation losses for a fundamental TE and TM modes versus grating pitch are shown in Fig. 4(d). The propagation loss of this 3-D HWG is larger than that of slab HWG discussed in the previous section. In case of the 3-D HWG, the propagation losses for TE and TM modes are also the lowest near  $\Lambda = 1.2 \mu\text{m}$ . The propagation loss at the parameters of “set A” is 2.2 dB/cm while it is 10.2 dB/cm for TM mode. The calculated polarization dependence loss (PDL) is 8 dB/cm. The polarization dependence of HWG can be controlled by varying the grating parameters. Fig. 4(e) shows the birefringence control by grating thickness. The calculated birefringence is lowest,  $5 \times 10^{-4}$  for same “set A.” A small enough value of birefringence  $5 \times 10^{-4}$  can be obtained without using phase matching layer [16]. Also, the fabrication tolerance of propagation loss as well as birefringence is large enough to withstand standard variation in grating parameters.

## 6. Fabrication and Characterization of HWG

The schematic of the fabricated HWG is shown in Fig. 5(a). The structure consists of a DBR mirror with vertical periodicity at the bottom having 5 pairs of Si/SiO<sub>2</sub> and an HCG mirror with lateral periodicity at

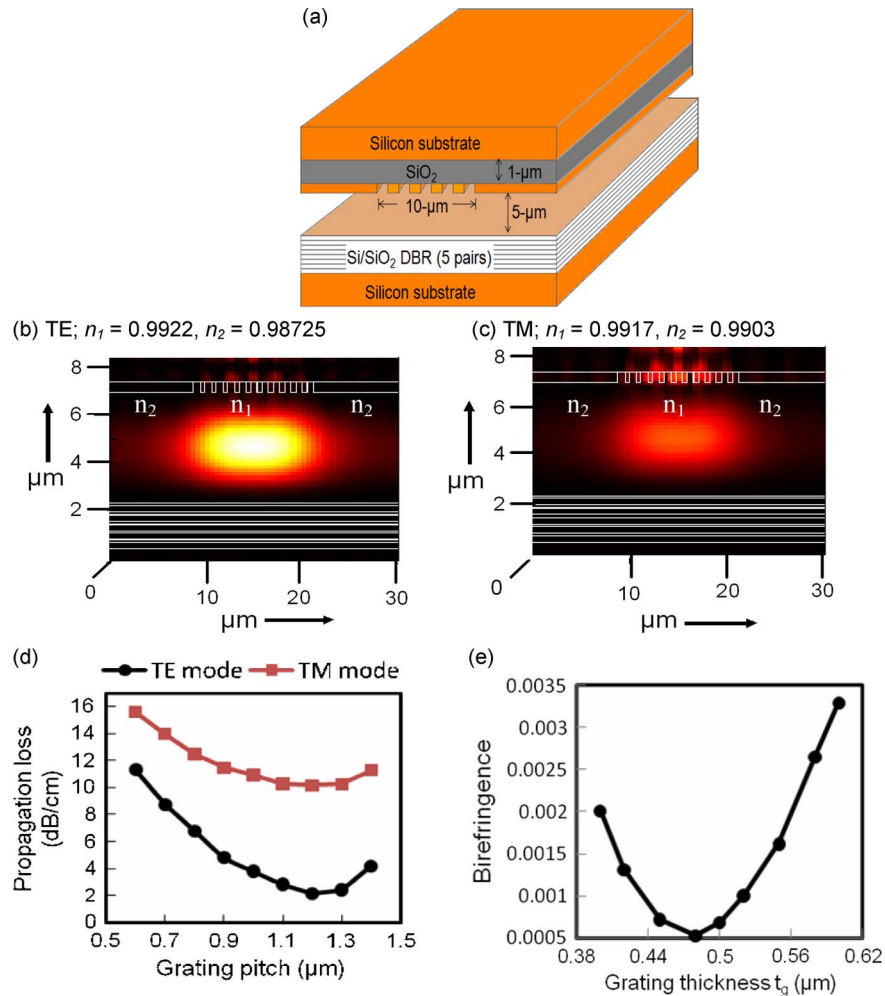


Fig. 4. (a) Schematic of 3-D HWG with a patterned HCG, (b) and (c) calculated mode field distributions, respectively, for TE and TM modes, at "set A" parameters, where  $n_1 > n_2$ , (d) propagation loss versus pitch at  $D = 5 \mu\text{m}$ ,  $t_g = 0.45 \mu\text{m}$ , and (e) effect of grating thickness on birefringence at  $D = 5 \mu\text{m}$ , grating pitch  $\Lambda = 1.2 \mu\text{m}$ , and  $C = 0.41$ .

the top. The bottom DBR mirror is loaded with SU-8 spacers. The quarter-wavelength-thick layers Si/SiO<sub>2</sub> (5 pairs) as a DBR mirror were deposited on a silicon substrate by electron beam evaporation. On the DBR mirror, 5- $\mu\text{m}$ -thick SU-8 spacers have been partly formed using standard photolithography. The distance between the pillars is 300  $\mu\text{m}$  and that is why these pillars have negligible impact on propagation characteristics. The air-core thickness of the HWG is fixed by the SU-8 spacer layer thickness on the DBR mirror. The HCG mirror on the top was formed in an SOI wafer having 1- $\mu\text{m}$ -thick SiO<sub>2</sub> and 0.45- $\mu\text{m}$ -thick silicon layer. The Si/air grating was fabricated by electron beam lithography followed by dry etching. The SEM top view of the fabricated HCG is shown in the inset of Fig. 5(a). All the waveguide parameters are from "set A." The bottom DBR mirror loaded with SU-8 spacers was then bonded onto the top HCG mirror to form the HWG with vertical and lateral periodicity. The measured near-field pattern is shown in Fig. 5(b) where we observed vertical and lateral optical confinement.

The propagation loss of the HWG for TE mode was measured using a cut-back method. We fabricated HWGs with various lengths. The measured propagation loss versus waveguide length is shown in Fig. 6(a). The measured propagation loss estimated from Fig. 6(a) is 4.2 dB/cm while the calculated propagation loss of the same structure of Fig. 4(a) is 2.2 dB/cm from Fig. 4(d). The measured propagation loss is larger than its calculated value which may be because of the

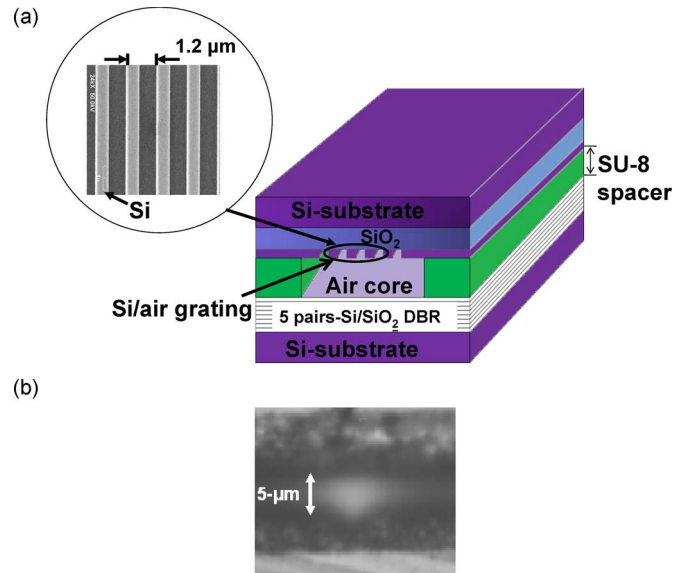


Fig. 5. (a) Schematic of fabricated 3-D HWG with a patterned HCG, shown in inset, and (b) measured near-field pattern showing cross section and optical confinement of the HWG.

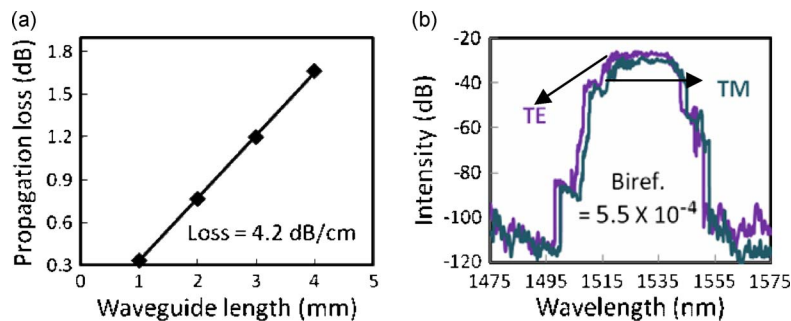


Fig. 6. (a) Measured propagation loss for TE mode by cut-back method and (b) reflected spectrum of grating loaded HWG, grating acts as a reflecting element, showing measured birefringence. The parameters used are from "set A."

fabrication errors including imperfect DBR layer thickness, imperfect HCG parameters or surface roughness inside an air core. In a separate experiment, we also measured the insertion losses for TE and TM modes for a 3-mm-long waveguide. The measured insertion losses for TE and TM modes are 1.2 dB and 3.8 dB, respectively and thus the measured PDL is 8.7 dB/cm which is not low enough, but would be acceptable for millimeter-long devices. Further optimizations of the HCG structure to reduce a TM mode loss are under progress. We found that the reduction in a HCG thickness and introducing a phase matching layer in a DBR [16] can reduce the TM mode loss and hence a lower PDL can be expected. Our calculations show that at  $t_g = 350$  nm and a phase matching layer of 56 nm, the propagation loss of a TM mode is 4.5 dB/cm while that of a TE mode is 2.7 dB/cm; the calculated PDL, thus, is 1.8 dB/cm with a birefringence of  $1.7 \times 10^{-4}$ . Further reduction of both PDL and the birefringence can be expected by optimizing the grating parameters of HCG.

To measure the birefringence of the HWG we form a  $\text{SiO}_2$  grating on the DBR mirror which acts as a reflecting element as described in [12]. The birefringence is given by  $B = (n_{\text{TE}} - n_{\text{TM}})/n_{\text{TE}}$  where  $n_{\text{TE}}$  and  $n_{\text{TM}}$  are effective indices of TE and TM modes, respectively. The Bragg wavelength is given by  $\lambda = 2n\Lambda$  where  $\Lambda$  is grating pitch. The birefringence can be estimated directly from Bragg wavelengths of TE and TM modes as the Bragg wavelength is proportional to effective index [12]. The grating reflectivity would also be affected by the imaginary part of the effective index. However, this effect can



be neglected since the imaginary part is  $10^3$  times smaller than that of the real part. Also, the birefringence in terms of Bragg wavelength can be given by  $B = (\lambda_{TE} - \lambda_{TM})/\lambda_{TE}$ , where  $\lambda_{TE}$  and  $\lambda_{TM}$  are the Bragg wavelength for TE and TM fundamental modes, respectively. The measured reflected spectrum of the fabricated 3-mm-long HWG with a  $\text{SiO}_2$  grating is shown in Fig. 6(b). The central peak wavelength for TE mode is 1527.8 nm while that for TM mode is 1527 nm which corresponds to a birefringence of  $5 \times 10^{-4}$ , which is in agreement with the calculated result for  $t_g = 0.48 \mu\text{m}$  as shown in Fig. 4(e). Thus the thickness of the silicon layer on SOI wafer may be  $0.48 \mu\text{m}$  instead of  $0.45 \mu\text{m}$ . Although the grating itself used as a reflecting element may cause a birefringence, the grating would make small contribution to the measured birefringence of the HWG. Our previous study [22] shows that the calculated birefringence of HWGs is in agreement with the measured birefringence of grating loaded HWGs.

## 7. Conclusion

In conclusion, an HWG with vertical and lateral periodicity has been proposed and numerical simulation results have been presented. A strong optical confinement can be achieved with the proposed HWG. The combination of DBR and HCG mirrors enables us to reduce the birefringence even at narrow air cores. A patterned HCG leads to strong lateral confinement in HWGs. An acceptable low propagation loss of TE mode for millimeter-long devices has been obtained theoretically and experimentally. Also, small birefringence of the order of  $10^{-4}$  has been demonstrated. With the further structural optimizations, the proposed structure can be used with narrower air cores to realize widely tunable photonic devices with low polarization dependence and low temperature sensitivity. There is a strong possibility of realization of the polarization insensitivity with HCG HWG. Further research on the utilization of unique properties of HWG and HCG is in progress. With the collaboration of HCG and the inherent properties of HWGs such as temperature insensitivity and wide tuning, it will be possible to design novel optical functions with large design tolerances.

## Acknowledgment

The authors thank A. Lakhani for his assistance in wafer bonding and Bala Pesala for waveguide measurements and helpful discussions.

---

## References

- [1] Y. Saito, T. Kanaya, A. Nomura, and T. Kano, "Experimental trial of using a hollow core waveguide as an absorption cell of concentration measurement of  $\text{NH}_3$  gas with a  $\text{CO}_2$  laser," *Opt. Lett.*, vol. 18, no. 24, pp. 2150–2152, Dec. 1993.
- [2] T. Delonges and H. Fouckhardt, "Integrated optical detection cell based on Bragg reflecting waveguides," *J. Chromatogr. A*, vol. 716, no. 1/2, pp. 135–139, Nov. 1995.
- [3] A. Grosse, M. Grewe, and H. Fouckhardt, "Deep wet etching of fused silica glass for hollow capillary optical leaky waveguides in microfluidic devices," *J. Micromech. Microeng.*, vol. 11, no. 3, pp. 257–262, May 2001.
- [4] S. Campopiano, R. Bernini, L. Zeni, and P. M. Sarro, "Microfluidic sensor based on integrated optical hollow waveguides," *Opt. Lett.*, vol. 29, no. 16, pp. 1894–1896, Aug. 2004.
- [5] W. Yang, D. B. Conkey, B. Wu, D. Yin, A. Hawkins, and H. Schmidt, "Atomic spectroscopy on a chip," *Nat. Photon.*, vol. 1, no. 6, pp. 331–335, 2007.
- [6] R. M. Jenkins, M. E. McNie, A. F. Blockley, N. Price, and J. MaQuillan, "Hollow waveguides for integrated optics," in *Proc. OECC/COIN*, 2004, pp. 900–901, 16F1-5.
- [7] P. Yeh and A. Yariv, "Bragg reflection waveguides," *Opt. Commun.*, vol. 19, no. 3, pp. 427–430, Dec. 1976.
- [8] M. Ibanescu, Y. Fink, S. Fan, E. L. Thomas, and J. D. Joannopoulos, "The coaxial omniguide—A novel all-dielectric waveguide," *Science*, vol. 289, pp. 415–419, 2000.
- [9] M. A. Duguay, Y. Kokubun, T. Koch, and L. Pfeiffer, "Antiresonant reflecting optical waveguides in  $\text{SiO}_2$ -Si multilayer structures," *Appl. Phys. Lett.*, vol. 49, no. 1, pp. 13–15, Jul. 1986.
- [10] S. G. Johnson, M. Ibanescu, M. Skorobogatiy, O. Weisberg, T. D. Engeness, M. Soljacic, S. A. Jacobs, J. D. Joannopoulos, and Y. Fink, "Low-loss asymptotically single-mode propagation in large-core OmniGuide fibers," *Opt. Express*, vol. 9, no. 13, pp. 748–779, Dec. 2001.
- [11] T. Miura, F. Koyama, Y. Aoki, A. Matsutani, and K. Iga, "Propagation characteristics of hollow waveguide for temperature-insensitive photonic integrated circuits," *Jpn. J. Appl. Phys.*, vol. 40, pp. L688–L690, 2001.
- [12] Y. Sakurai and F. Koyama, "Tunable hollow waveguide distributed Bragg reflectors with variable air core," *Opt. Express*, vol. 12, no. 13, pp. 2851–2856, Jun. 2004.
- [13] M. Kumar, T. Sakaguchi, and F. Koyama, "Giant birefringence and tunable differential group delay in Bragg reflector based on tapered three dimensional hollow waveguide," *Appl. Phys. Lett.*, vol. 94, no. 6, p. 061112, Feb. 2009.

- [14] T. Badreldin, K. Madkour, and D. Khalil, "Design of silicon hollow waveguide in-line polarizer using a photonic crystal concept," *J. Opt. A, Pure Appl. Opt.*, vol. 9, no. 1, pp. 88–94, Jan. 2007.
- [15] T. Miura and F. Koyama, "Low-loss semiconductor hollow waveguide with GaAs/AlAs multilayer mirrors for widely tunable waveguide devices," in *Proc. 16th Annu. Meeting IEEE Laser Electro-Opt. Soc.*, Oct. 2003, pp. 838–839, ThH4.
- [16] M. Kumar, T. Sakaguchi, and F. Koyama, "Tunable 3D nanostep hollow waveguide with low polarization dependence," *Appl. Phys. Express*, vol. 1, p. 052002, 2008.
- [17] M. C. Y. Huang, Y. Zhou, and C. J. Chang-Hasnain, "A surface-emitting laser incorporating a high-index-contrast subwavelength grating," *Nat. Photon.*, vol. 1, no. 2, pp. 119–122, 2007.
- [18] R. Magnusson and M. Shokooch-Saremi, "Physical basis for wideband resonant reflectors," *Opt. Express*, vol. 16, no. 5, pp. 3456–3462, Mar. 2008.
- [19] Y. Zhou, V. Karagodsky, B. Pesala, F. G. Sedgwick, and C. J. Chang-Hasnain, "A novel ultra-low loss hollow-core waveguide using subwavelength high-contrast gratings," *Opt. Express*, vol. 17, no. 3, pp. 1508–1517, Feb. 2009.
- [20] M. G. Moharam and T. K. Gaylord, "Rigorous coupled-wave analysis of planar-grating diffraction," *J. Opt. Soc. Amer.*, vol. 71, no. 7, pp. 811–818, Jul. 1981.
- [21] A. S. Sudbo, "Film mode matching: A versatile numerical method for vector mode field calculations in dielectric waveguides," *Pure Appl. Opt.*, vol. 2, no. 3, pp. 211–233, May 1993.
- [22] M. Kumar, T. Sakaguchi, and F. Koyama, "Wide tunability and ultralarge birefringence with 3D hollow waveguide Bragg reflector," *Opt. Lett.*, vol. 34, no. 8, pp. 1252–1254, Apr. 2009.